Available online at www.sciencedirect.com
ScienceDirect
Journal of Bionic Engineering 9 (2012) 367–376

Cuttlebone: Characterisation, Application and Development of Biomimetic Materials

Joseph Cadman[1], Shiwei Zhou[2], Yuhang Chen[3], Qing Li[1]

1. *School of Aerospace, Mechanical and Mechatronic Engineering, The University of Sydney, NSW* 2006, *Australia*
2. *Innovative Structures Group, School of Civil, Environmental and Chemical Engineering, RMIT University, GPO Box* 2476, *Melbourne* 3001, *Australia*
3. *School of Engineering and Physical Sciences, Heriot-Watt University, Edinburgh EH14 4AS, UK*

Abstract

Cuttlebone signifies a special class of ultra-lightweight cellular natural material possessing unique chemical, mechanical and structural properties, which have drawn considerable attention in the literature. The aim of this paper is to better understand the mechanical and biological roles of cuttlebone. First, the existing literature concerning the characterisation and potential applications inspired by this remarkable biomaterial is critiqued. Second, the finite element-based homogenisation method is used to verify that morphological variations within individual cuttlebone samples have minimal impact on the effective mechanical properties. This finding agrees with existing literature, which suggests that cuttlebone strength is dictated by the cuttlefish habitation depth. Subsequently, this homogenisation approach is further developed to characterise the effective mechanical bulk modulus and biofluidic permeability that cuttlebone provides, thereby quantifying its mechanical and transporting functionalities to inspire bionic design of structures and materials for more extensive applications. Finally, a brief rationale for the need to design a biomimetic material inspired by the cuttlebone microstructure is provided, based on the preceding investigation.

Keywords: cuttlebone, characterisation, biomimetic, homogenisation

doi: 10.1016/S1672-6529(11)60132-7

1 Introduction

Cuttlebone functions both as the rigid structural component of the cuttlefish body and as a buoyancy tank for the cuttlefish, providing an efficient means of minimising the effort required to maintain its vertical position in the sea[1]. A gas and liquid mixture is used to regulate the pressure inside the cuttlebone via an osmotic process[2,3], allowing the cuttlefish to maintain its neutral buoyancy. To fulfil these highly sophisticated and mixed functional requirements, the cuttlebone needs to possess high stiffness, high porosity and high permeability. Physically, these are competing properties as the stiffness of a porous material can generally be increased by adding more material; but too much material jeopardises both buoyancy and permeability. The cuttlebone microstructure balances these competing multi-functionalities perfectly.

1.1 Characterisation: physical, chemical and mechanical properties

Cuttlebone signifies a special class of ultra-lightweight, high stiffness and high permeability cellular biomaterials, providing the cuttlefish with an efficient means of maintaining neutral buoyancy at considerable habitation depths[1,3]. In addition, this rigid cellular material provides the structural backbone of the body and plays a key role in the protection of vital organs[1,2]. The cuttlebone has two main components: the dorsal shield and the lamellar matrix (Fig. 1). The dorsal shield is very tough and dense, providing a rigid substrate for protection, structure and the development of the lamellar matrix of cuttlebone[1,2]. The lamellar matrix of cuttlebone has an extreme porosity (up to 90%), but also manages to withstand very high hydrostatic

The original paper was presented in the International Bionic Engineering Conference 2011 (IBEC2011), Sept. 18-20, Boston, USA. This revised version is recommended for publication by Professor Julian Vincent, the chair of IBEC2011.

Corresponding author: Qing Li
E-mail: Qing.Li@Sydney.edu.au

pressure. The lamellar matrix consists primarily of aragonite (a crystallised form of calcium carbonate, $CaCO_3$), enveloped in a layer of organic material[1,2,4] composed primary of β-chitin[5]. The organic layer entirely envelopes the inorganic ceramic, and is thought to initiate, organise and inhibit the mineralisation of the inorganic material[1,5]. From a mechanical perspective, the organic layer is also thought to provide a certain toughening effect to the material[1]. Studies for other rigid marine materials with similar chemical characteristics, such as nacre, have highlighted this toughening effect of the organic material by investigating their energy absorption mechanisms[6–11].

Scanning Electron Microscopy (SEM) images of the lamellar matrix of cuttlebone reveal a layered, cellular quasi-periodic microstructure consisting of lamellae (or septa) separated by pillars (Fig. 1). The pillars form channels of approximately uniform width which progress through the material along a meandering, convoluted path (Fig. 2a). The degree of convolution is recognized as having an influence on the compressive strength of the material [1,2]. These channels also tend to display a high degree of connectivity (Fig. 2a).

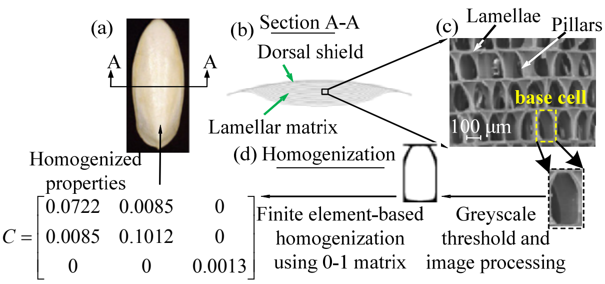

Fig. 1 Cuttlebone images showing: (a) planar view of cuttlebone (dorsal side); (b) schematic of cuttlebone cross section (section A-A) with dorsal shield and lamellar matrix labelled; (c) detail of lamellar matrix transverse cross section and (d) image-based finite element modeling for homogenization.

There is a large degree of difference in lamella height, pillar spacing and channel convolution between different species, different individuals of the same species, and even in different areas of a single cuttlebone sample (Fig. 2b). These variations are reported as being dependent on the health and environment of an individual cuttlefish, as much as its specific functional requirements[1,2,4,12–14]. These factors can manifest in the cuttlebone morphology in a number of unique ways, including changes in lamella and pillar spacing. Empirical results from Ward and Boletzky[14] found that undernourished cuttlefish subjected to environmental stress could develop significantly stronger cuttlebones with reduce lamellae and pillar spacing. Also, Boletzky[12] observed that changes in morphology in the same cuttlebone may be due to the development of portions of the cuttlebone through different seasons, i.e. decreased height between lamella corresponds to regions that developed during the winter months.

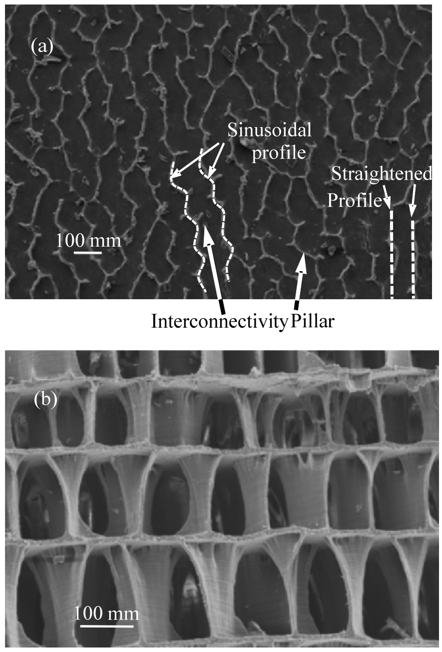

Fig. 2 Cuttlebone images showing: (a) channels formed by convoluted pillar formation with examples of sinusoidal and straightened profiles highlighted; and (b) transverse cross section clearly displaying morphological variations.

The layered microstructure of the cuttlebone has been shown to collapse in a controlled, layer-by-layer fashion under excess compressive loading. This means that the cuttlefish can descend below the depth limit of its cuttlebone for limited periods of time without catastrophic damage[1,2]. In this context, Ward and Boletzky[14] showed that some cuttlefish species could survive after partial collapse of the cuttlebone and that the formation of new layers after this type of collapse was fairly rapid.

The permeability of the cuttlebone lamellar matrix is another important factor as the cuttlefish relies on adjusting the liquid-gas mixture to regulate the internal pressure and maintain its neutral buoyancy[2,3]. The isolation of the individual layers is also important in this instance as the failure of any single layer will not flood the whole cuttlebone or affect the permeability of neighbouring layers[1,2,14]. Despite its importance to the functionality of cuttlebone, the permeability of the cuttlebone has not been explored in detail in the literature to date. A method for determining the permeability of cuttlebone using the finite element-based homogenization method will be introduced below.

1.2 Existing predictive models for cuttlebone strength

There is a great variety in the morphology of cuttlebones due primarily to the large range of species inhabiting the oceans. Research has been conducted into correlating cuttlebone strength with known habitation depth information obtained from empirical records, with a reasonable degree of success[2,4]. The predictive models are based around the possible failure criteria of the structural features of cuttlebone, including buckling of the pillars[2], or plate failure of the lamellae[4]. Given the significant variation in the cuttlebone morphology of different species, it is reasonable to assume that the different models are best applied to individual cuttlebones depending on such considerations as layer height (higher pillars are more prone to buckling), and pillar spacing (wider pillar spacing will increase the likelihood of collapse via one of the plate failure criteria)[4].

However, these failure models tend not to be as accurate when considering the habitation depths of deep sea species of cuttlefish, frequently predicting habitation depths significantly shallower than fishery records would indicate[2,4]. Such discrepancies highlight the critical importance of material distribution under increasing hydrostatic loads, as noted by Sherrard[4] who found that slight inaccuracies measuring geometrical features had a significant impact on the magnitude of the habitation depth calculations.

Gower and Vincent[2] hypothesised that such predictive models may only provide reasonable predictions up to 240 m, i.e. the theoretical buoyancy limit of the cuttlebone, beyond which the pressure differential between the cuttlefish blood and fresh water is equal to the hydrostatic pressure of the sea, leading to the breakdown of the osmotic pumping process[15]. Beyond this limit, they suggested that the cuttlefish must surrender its neutral buoyancy by letting body fluids enter the cuttlebone in order to avoid implosion under increasing hydrostatic pressure. Conversely, to avoid explosion due to expanding gases upon return to the buoyancy limit, the fluid is rapidly pumped back out again. Therefore, in this scenario, the role of permeability becomes critically important to the functional requirements of the cuttlebone.

1.3 Applications

Due to the unique physical, chemical and mechanical characteristics of this natural cellular material, a range of novel applications for the material have recently been investigated.

Cuttlebone has been proposed as a suitable raw material for a range of applications. For instance, Poompradub *et al*.[16] investigated the potential for using ground cuttlebone as a filler for natural rubber. It was found that ground cuttlebone provided comparable mechanical properties to commercially available fillers, even though it was significantly less refined. This was thought to be due to the organic component (β-chitin) promoting interaction between the natural rubber and inorganic aragonite of cuttlebone.

Yildirim *et al*.[17] have investigated the compatibility of raw cuttlebone with human bone tissue. They found that the mineral composition of cuttlebone is compatible with human bone tissue and suggested that the direct use of cuttlebone as a bone tissue scaffold warranted further investigation. In addition, Garcia-Enriquez *et al*.[18] and Jasso-Gastinel *et al*.[19] investigated the use of cuttlebone as a filler in acrylic bone cements and found enhanced osseointegration and no evidence of secondary infection during *in vivo* testing with rabbits. The mechanical properties of the bone cement with up to 30% cuttlebone filler were found to be comparable to those of the commercial bone cement, and well within the accepted standards for bone cements.

Another approach for using cuttlebone in tissue scaffolding applications revolves around the hydrothermal transformation of aragonite into hydroxyapatite, a ceramic which is already deemed appropriate for bone tissue engineering applications[20–22]. Rocha *et al*.[23–25] and Kannan *et al*.[26] used hydrothermal transformation to produce hydroxyapatite tissue scaffolds retaining the cuttlebone architecture, noting that the channel sizes of the cuttlebone samples investigated were considered beneficial for bone ingrowth (~100 × 200 μm). Their studies included tests for biocompatibility with osteoblasts, whose viability was enhanced by the presence of the scaffolds. A range of other benefits including good machinability and fluoride substitution for dental applications are also recognized, indicating rather promising results.

However, it is noted that the existing work has not investigated the strength of the final product, only stating that the scaffolds were "strong enough to be safely handled"[25,26]. It is also noted in these studies that other natural materials (like nacre and coral) generally collapse after hydrothermal transformation[27]. It is therefore reasonable to infer that the advantageous mechanical properties of cuttlebone may be negatively affected during this chemical process. The large range in cuttlebone morphology is also not considered in their discussion, a factor which may also impact on the direct use of such scaffolds in applications where mechanical properties are an important concern[28].

Another promising application of the direct use of cuttlebone is as a template for creating superior superconducting materials. Culverwell *et al*.[29] found that the porous, permeable microstructure of cuttlebone not only aided in fabricating the superconductor, but also increased the critical current density by two orders of magnitude over existing commercial solutions. Nevertheless, a lack of strength in the final product was a significant issue again. Although silver doping was used to increase the materials strength, this reduced the superconducting performance considerably. How to achieve the desired performance while retaining material strength and structure represents a major problem in such chemical transformations and fabrication processes.

Cuttlebone powder has also been mixed with phosphoric acid to synthesise calcium phosphate, a ceramic known to have potential in bone tissue engineering applications[30]. The process is compared favorably to a similar study which produced biocompatible and easily sintered calcium phosphate powders by mixing egg shells and phosphoric acid[31]. These simple and inexpensive procedures are good candidates for the mass production of calcium phosphate ceramics for biomedical applications, including bone tissue scaffolds.

Cuttlebone has also been used as an organic matrix for the formation of silver and gold nano-particles[32–34] for using in novel applications. The cuttlebone was dematerialized in a hydrochloric acid and the organic component of the structure used to grow nano-particles. The size and distribution of the nano-particles were influenced by the protein component in the cuttlebone derived organic matrix. The organic matrix of cuttlebone has also been proposed as a suitable template for the mineralization of chitin-silica composites[35]. The potential for using the organic component of cuttlebone in biomedical applications has also been examined in terms of cell adhesion and growth. Cuttlebone and shrimp shell derived chitosan displayed good biocompatibility, supporting cell attachment and growth[36]. It is noted that the original cuttlebone architecture is not maintained in these studies due to the demineralization process.

1.4 Current research

The authors have recently attempted to characterize the effective stiffness of the cuttlebone using two-dimensional (2D) finite element-based homogenisation methods[37,38] (Fig. 1d). This method allows the calculation of the effective mechanical properties of a periodic microstructural material based on the morphology of a single 2D base cell or Representative Volume Element (RVE)[39]. Since the transverse cross section of cuttlebone is quasi-periodic, this method can be used to provide an approximation to the effective mechanical properties with a reasonable degree of accuracy[40]. Simple extensions of this methodology have also provided an alternative means for quantifying the vast array of material properties available in different cuttlebone samples[28,41,42].

The remainder of this paper will briefly explore the impact of morphological variations on the effective stiffness of the lamellar matrix of cuttlebone and further extend the homogenization algorithm from 2D stiffness to 3D bio-transport properties for such a cellular microstructure inspired by the cuttlebone.

2 Methods and materials

2.1 Image extraction process

The image extraction process (Fig. 1d) developed by the authors[37,38], is used in this study, allowing the material distribution to be replicated as closely as possible. This method involves cropping the original SEM image to a single RVE model and applying a grey-scale threshold to convert the image into a void-solid (0 – 1 matrix) representation that can be used directly in the finite element-base homogenization formulation.

Two different cuttlebone specimens were used in this study, referred to herein as Cuttlebone 1 and Cuttlebone 2 (Fig. 3). Cuttlebone 1 was a smaller cuttlebone with a macroscopic length of approximately 100 mm and microstructural lamella spacing around 100 µm – 200 µm in height and pillar spacing around 80 µm – 100 µm wide (Fig. 3a). The second sample (Cuttlebone 2) was a larger cuttlebone with a macroscopic length of approximately 195 mm, with lamella spacing around 200 µm – 350 µm and pillar spacing around 60 µm – 100 µm wide (Fig. 3b). Additional organic layers (the intercameral lamellae referred to Ref. [2]) are also present within the microstructural base cells of Cuttlebone 2. These differences suggest that Cuttlebone 2 is taken from a cuttlefish with a significantly shallower habitation depth[2]. Whether the results reflect this will be explored as part of this study.

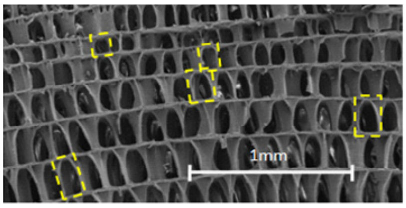

(a)

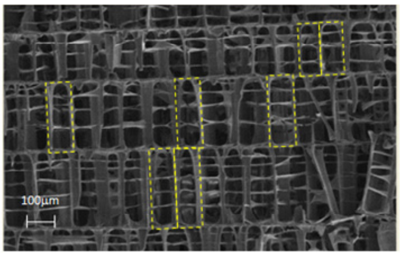

(b)

Fig. 3 SEM images displaying morphological variations for two different samples of: (a) Cuttlebone 1 and (b) Cuttlebone 2, with extracted RVEs outlined.

2.2 Homogenization method

The homogenization method calculates the effective mechanical properties based on the property and distribution of base materials within a RVE. The effective stiffness tensor, C^H_{ijkl} can be formulated as[39,43]

$$C^H_{ijkl}(\rho) = \frac{1}{|\Omega|}\int_\Omega C_{ijmn}(\rho)\left[\varepsilon^{0(kl)}_{mn} - \varepsilon^{*(kl)}_{mn}\right]\mathrm{d}\Omega, \quad (1)$$

where $|\Omega|$ denotes the area of the RVE, Ω. C_{ijmn} denotes the stiffness tensor of the base material, assumed isotopic[38,39,44,45]. The volume fraction of solid phase is denoted by ρ, where the solid and void elements are designated $\rho = 1$ and $\rho = 0$, respectively. The characteristic strain fields $\varepsilon^{*(kl)}_{mn}$ are obtained by solving the characteristic equation:

$$\int_\Omega C_{ijmn}\varepsilon_{ij}(v)\varepsilon^{*(kl)}_{mn}\mathrm{d}\boldsymbol{x} = \int_\Omega C_{ijmn}\varepsilon_{ij}(v)\varepsilon^{0(kl)}_{mn}\mathrm{d}\Omega, \quad (2)$$

where the virtual displacement field $v \in H_{per}$ belongs to the periodic Sobolev functional space[46,47]. In the present study, a Poisson's ratio of 0.25 was used for the base material[2] and a normalized Young's modulus of 1 unit was assigned to the base material in order to obtain dimensionless results for a bioinspired design purpose.

The bulk modulus is a measure of a material's capacity to withstand a unit hydrostatic strain, and is therefore considered relevant and applicable to cuttlebone due to its habitation in a marine environment. Bulk modulus is calculated as[47],

$$B^H = \frac{1}{n^2}\sum_{a,b=1}^{n} C^H_{aabb}, \quad (3)$$

where C^H_{aabb} are the components of the effective orthotropic elasticity tensor and $n = 2$ for 2D problems and $n = 3$ for 3D problems.

It is only meaningful to approximate the effective transport properties in 3D because such a cellular material ideally prevents flow across solid lamellae and pillar boundaries in the structures explored. In general, the effective permeability, κ, can be formulated as Ref. [48]

$$\kappa^H_{ij}(\rho) = \frac{1}{|\Omega|}\int_\Omega \kappa^e_{ij}(\rho)\left[I - \frac{\partial \chi_i}{\partial y_j}\right]\mathrm{d}\Omega, \quad (4)$$

where I is the identity matrix, κ^H_{ij} and κ^e_{ij} are the homogenized and elemental transport properties and χ_i denotes the solution to the following characteristic transport equation,

$$\frac{\partial}{\partial x_i}\left(\kappa\frac{\partial \chi}{\partial x_j}\right) = \frac{\partial \kappa}{\partial x_i}. \quad (5)$$

To obtain dimensionless results, $\kappa^e = 1$ for void material and $\kappa^e = 0$ for solid material. It is noted that other approaches can also be employed to characterize the effective permeability of Navier Stokes flow through porous media, e.g.[49,50], but are not considered in this work.

3 Results and discussion

3.1 Effect of morphological changes

As mentioned above, significant morphological changes can occur within an individual cuttlebone sample (Figs. 2 and 3). It is reasonable to assume that such morphological variations may result in different mechanical and bio-transport properties being predicted in different RVEs. However, it is also expected that the effective bulk modulus results calculated from any location within a single cuttlebone will lie within a relatively narrow range, indicative of the typical habitation depth of the cuttlebone species[2]. Theoretically, this can also be related to material bounds, which typically constrain the possible range of material properties for a certain volume fraction[51–53].

To explore the effect of such morphological variations within individual cuttlebone samples, the effective bulk modulus is calculated for the lamellar matrix based on a number of morphologically different RVEs extracted from SEM images of the transverse cross section (Fig. 3).

Fig. 4 plots the variation of bulk modulus against the aspect ratio of the various extracted RVEs for two cuttlebone samples (Cuttlebone 1 and Cuttlebone 2). Mean values and the standard deviations of the results are also included, permitting some observations regarding the distribution of the bulk modulus. It is observed that the results in both cases lie within a fairly narrow band of values; the standard deviation is approximately ±7% (i.e. the bulk modulus remains fairly constant, somewhat independent of the aspect ratio). Also, the bulk modulus for Cuttlebone 1 is approximately twice the bulk modulus of Cuttlebone 2. This elevated bulk modulus implies that Cuttlebone 1 can withstand greater hydrostatic pressures, confirming the earlier observation (section **2.1**) that this cuttlebone sample is taken from a cuttlefish that can inhabit greater depths. Finally, it is noted that the spread of measured aspect ratios is far wider for Cuttlebone 2, which supports the suggestion by Gower and Vincent[2] that cuttlefish living at greater depths enjoy a more stable environment and are not affected by severe seasonal changes as much as species inhabiting shallower waters[12].

It is noted that the image extraction process (Fig. 1d), whilst potentially permitting a very accurate rendering of the RVE topology, is also quite subjective, depending on appropriate image processing parameters being used. Sherrard[4] found that slight errors in the measured wall thicknesses led to a marked impact on the calculated results and this is also reflected in the current methodology. To illustrate this phenomenon, Fig. 5 shows two binary RVEs which both approximate the same original SEM image. The overall topology and shape are nearly identical in both cases; the only difference being that the pillars are marginally thicker in the second version (low row in Fig. 5). This slight difference in the definition of the pillars leads to an increase in the bulk modulus of around 29%.

Given this potential for inaccuracy in the image extraction process, the results of Fig. 5 provide some support for the assumption that all the layers of a cuttlebone sample will possess a similar stiffness indicative of the standard range of habitation depth for the cuttlefish species[2,4]. However, it is noted that greater control over the image processing procedure would allow for a more standardized image extraction procedure and could provide more consistent results and confident conclusions.

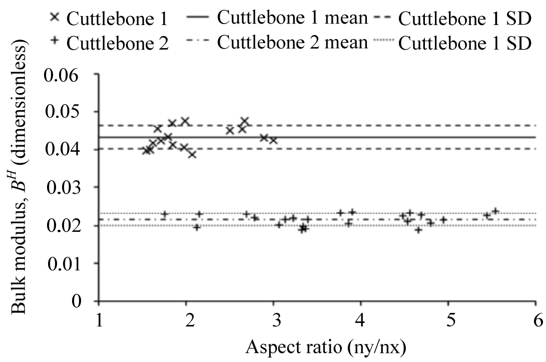

Fig. 4 Bulk modulus plotted against aspect ratio of extracted RVEs for Cuttlebone 1 and Cuttlebone 2, including raw data, mean and Standard Deviation (SD).

Binary base cell	Homogenized stiffness tensor(dimensionless)
	$C^H = \begin{bmatrix} 0.0227 & 0.0019 & 0 \\ 0.0019 & 0.0351 & 0 \\ 0 & 0 & 0.0005 \end{bmatrix}$ B^H=0.0152
	$C^H = \begin{bmatrix} 0.0227 & 0.0021 & 0 \\ 0.0021 & 0.0513 & 0 \\ 0 & 0 & 0.0006 \end{bmatrix}$ B^H=0.0196

Fig. 5 The effect of slight topological differences on stiffness tensor and bulk modulus.

3.2 Cuttlebone permeability

The importance of permeability to the functional requirements of cuttlebone is outlined above. Moreover, in many of the applications for cuttlebone listed in section **1.3**, permeability is critical, e.g. tissue engineering scaffolds[23–26] and superconductor fabrication[29]. Therefore, the ability to characterize this effective property and use it in subsequent biomimetic design regimes is of considerable significance.

In this study, two simple 3D RVEs are created by extruding a 2D RVE topology (created via the image extraction process (Fig. 1d) along a straight profile and a sinusoidal profile (Fig. 2a), respectively (Fig. 6). The sinusoidal profile has a wavelength equal to the width and amplitude equal to 1/4 the width from a statistic observation on Fig. 2a. This creates two binary RVEs which are periodic in three dimensions and are therefore appropriate for analysis using the homogenization technique outlined above.

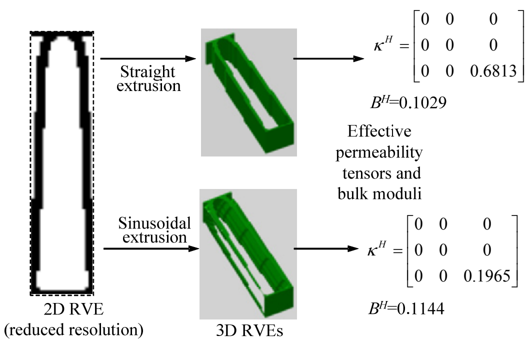

Fig. 6 3D RVEs created by extruding through different periodic profiles and their permeability tensors and bulk moduli.

The permeability and stiffness tensors for this 3D RVE are included in Fig. 6. It is immediately apparent that there is only permeability in the *z*-direction, with no fluid able to flow through the solid lamellae in the base cell. Also, it is clear that introducing curvature to the extrusion profile (lower part in Fig. 6) reduces the permeability by about 71%. In contrast, the added curvature leads to an increase of around 11% in bulk modulus. Permeability and stiffness are recognized as competing properties, making the precise material distribution of cuttlebone, which apparently optimizes both, all the more remarkable.

3.3 Motivations for a biomimetic material design

It is clear that the unique characteristics of this material structure make it a promising candidate for a number of novel applications. Indeed, some recent investigations have demonstrated significant merits and potentials. However, there are some limitations with applications that rely on maintaining the cuttlebone architecture. Firstly, the cuttlebone might lose a large amount of its stiffness via the chemical conversion processes adopted[23–26,29]. Secondly, the mechanical properties of cuttlebone may vary widely due to different functional requirements at different habitation depths (section **3.1**)[2], which may potentially lead to a degree of uncertainty in the mechanical properties[28,41,42]. In applications where stiffness and permeability are both critical, the ability to have precise control over the microstructural features appears critical. Additionally, the size of the final product is limited according to the size of the cuttlebone sample. It is also noted that larger cuttlebones generally belong to shallow water species which possess a relatively weaker cuttlebone due to the required functionality[2]. Finally, whilst the structural benefits of cuttlebone are apparent in its natural environment, it is unclear whether these advantages will transfer directly to other applications. Mayer[9] realised that natural cellular materials are optimized for a specific set of local conditions. Outside of this environment, changes need to be made for appropriate use. Such factors point to the development of a biomimetic material based on the cuttlebone microstructure.

In this bioinspired material, the microstructure and mechanical and biotransport properties could be finely controlled and potentially scaled to suit any application requiring lightweight, high stiffness, high compressive strength, and high permeability materials. This biomimetic material could be fabricated using Solid Free-form Fabrication (SFF) techniques (Fig. 7)[41,54,55]. The range of raw materials and SFF techniques available for use with such fabrication methods also increases flexibility as far as material properties are concerned[54,55].

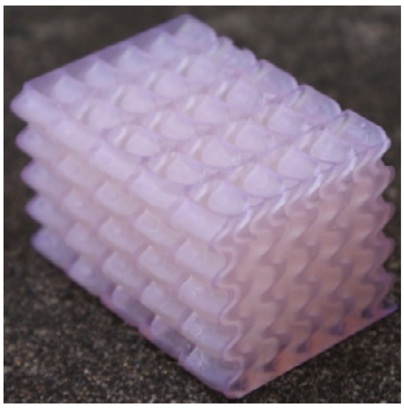

Fig. 7 Example of biomimetic material inspired by the microstructure of cuttlebone. Printed using Stereo Lithographic Apparatus (SLA), a common SFF technique (50 × original scale).

4 Conclusion

Cuttlebone is a lightweight, cellular material which has enjoyed some attention in the literature over the previous decades. In order to assess the current state of research into the characterization and potential advanced applications for this material, a critical review of the existing literature is presented in the first section of this paper. The existing chemical, physical and mechanical characterization of cuttlebone provides much insight into the microstructural architecture and function of the material. In addition, mathematical models have attempted to correlate cuttlebone stiffness to habitation depth, with some degree of success. It is shown that the finite element-based homogenization technique can also be used in this capacity. However, no attempt at characterizing the transport properties of cuttlebone exists in the literature to date. For the first time, the homogenization approach is adopted to approximate the permeability of cuttlebone using the finite element-based homogenization technique in this paper. A brief rationale for the development of biomimetic materials inspired by the cuttlebone microstructure, based on the preceding findings, concludes the paper.

Acknowledgments

The support from Australian Research Council (ARC) is great acknowledged. The first author also appreciates the Sydney University Postgraduate Award during his PhD study.

References

[1] Birchall J D, Thomas N L. On the architecture and function of cuttlefish bone. *Journal of Materials Science*, 1983, **18**, 2081–2086.

[2] Gower D, Vincent J F V. The mechanical design of the cuttlebone and its bathymetric implications. *Biomimetics*, 1996, **4**, 37–57.

[3] Vogel S. Living in a physical world VIII. Gravity and life in water. *Journal of Biosciences*, 2006, **31**, 309–322.

[4] Sherrard K M. Cuttlebone morphology limits habitat depth in eleven species of Sepia (Cephalopoda: Sepiidae). *The Biological Bulletin*, 2000, **198**, 404–414.

[5] Falini G, Fermani S. Chitin mineralization. *Tissue Engineering*, 2004, **10**, 1–6.

[6] Vincent J F V. Ceramics from invertebrate animals, in Levy M B (Ed.), *Handbook of Elastic Properties of Solids*, *Liquids and Gases*, Academic Press, New York, USA, 2001, 213–226.

[7] Liang Y, Zhao J, Wang L, Li F M. The relationship between mechanical properties and crossed-lamellar structure of mollusk shells. *Materials Science and Engineering a-Structural Materials Properties Microstructure and Processing*, 2008, **483–484**, 309–312.

[8] Jackson A P, Vincent J F V, Turner R M. Comparison of nacre with other ceramic composites. *Journal of Materials Science*, 1990, **25**, 3173–3178.

[9] Mayer G. New classes of tough composite materials– Lessons from natural rigid biological systems. *Materials Science and Engineering*: *C*, 2006, **26**, 1261–1268.

[10] Mayer G. Rigid biological systems as models for synthetic composites. *Science*, 2005, **310**, 1144–1147.

[11] Mayer G, Sarikaya M. Rigid biological composite materials: Structural examples for biomimetic design. *Experimental Mechanics*, 2002, **42**, 395–403.

[12] Boletzky S V. Sepia officinalis, in: Boyle P R (Ed.), *Cephalopod Life Cycles*, Academic Press, London, UK, 1983, 31–52.

[13] Gutowska M A, Melzner F, Portner H O, Meier S. Cuttlebone calcification increases during exposure to elevated seawater pCO2 in the cephalopod Sepia officinalis. *Marine Biology*, 2010, **157**, 1653–1663.

[14] Ward P D, Boletzky S V. Shell implosion depth and implosion morphologies in three species of Sepia (Cephalopoda) from the Mediterranean Sea. *Journal of the Marine Biological Association of the United Kingdom*, 1984, **64**, 955–966.

[15] Denton E J, Gilpinbrown J B, Howarth J V. The osmotic mechanism of cuttlebone. *Journal of the Marine Biological Association of the United Kingdom*, 1961, **41**, 351–363.

[16] Poompradub S, Ikeda Y, Kokubo Y, Shiono T. Cuttlebone as reinforcing filler for natural rubber. *European Polymer Journal*, 2008, **44**, 4157–4164.

[17] Yildirim O S, Okumus Z, Kizilkaya M, Ozdemir Y, Durak R, Okur A. Comparative quantative analysis of sodium, magnesium, potassium and calcium in healthy cuttlefish backbone and non-pathological human elbow bone. *Canadian Journal of Analytical Sciences and Spectroscopy*, 2007, **52**, 270–275.

[18] Garcia-Enriquez S, Guadarrama H E, Reyes-Gonzalez I, Mendizabal E, Jasso-Gastinel C F, Garcia-Enriquez B, Rembao-Boiorquez D, Pane-Pianese C. Mechanical performance and in vivo tests of an acrylic bone cement filled with bioactive sepia officinalis cuttlebone. *Journal of Biomaterials Science-Polymer Edition*, 2010, **21**, 113–125.

[19] Jasso-Gastinel C F, Enriquez S G, Flores J, Reyes-Gonzalez I,

Mijares E M. Acrylic bone cements modified with bioactive filler. *Macromolecular Symposia*, 2009, **283-284**, 159–166.

[20] Ivankovic H, Ferrer G G, Tkalcec E, Orlic S, Ivankovic M. Preparation of highly porous hydroxyapatite from cuttlefish bone. *Journal of Materials Science*: *Materials in Medicine*, 2009, **20**, 1039–1046.

[21] Ivankovic H, Tkalcec E, Orlic S, Ferrer G G, Schauperl Z. Hydroxyapatite formation from cuttlefish bones: kinetics. *Journal of Materials Science-Materials in Medicine*, 2010, **21**, 2711–2722.

[22] Kasioptas A, Geisler T, Putnis C V, Perdikouri C, Putnis A. Crystal growth of apatite by replacement of an aragonite precursor. *Journal of Crystal Growth*, 2010, **312**, 2431–2440.

[23] Rocha J H, Lemos A F, Agathopoulos S, Kannan S, Valério P, Ferreira J M. Hydrothermal growth of hydroxyapatite scaffolds from aragonitic cuttlefish bones. *Journal of Biomedical Materials Research - Part A*, 2006, **77**, 160–168.

[24] Rocha J H G, Lemos A F, Agathopoulos S, Valerio P, Kannan S, Oktar F N, Ferreira J M F. Scaffolds for bone restoration from cuttlefish. *Bone*, 2005, **37**, 850–857.

[25] Rocha J H G, Lemos A F, Kannan S, Agathopoulos S, Ferreira J M F. Hydroxyapatite scaffolds hydrothermally grown from aragonitic cuttlefish bones. *Journal of Materials Chemistry*, 2005, **15**, 5007–5011.

[26] Kannan S, Rocha J H G, Agathopoulos S, Ferreira J M F. Fluorine-substituted hydroxyapatite scaffolds hydrothermally grown from aragonitic cuttlefish bones. *Acta Biomaterialia*, 2007, **3**, 243–249.

[27] Zaremba C M, Morse D E, Mann S, Hansma P K, Stucky G D. Aragonite-hydroxyapatite conversion in gastropod (abalone) nacre. *Chemistry of Materials*, 1998, **10**, 3813–3824.

[28] Cadman J, Chen Y, Zhou S, Li Q. Bioinspired lightweight cellular materials - understanding effects of natural variation on mechanical properties. *Mater. Sci. Eng. C-Biomimetic Supramol. Syst.* 2012, *Submitted*.

[29] Culverwell E, Wimbush S C, Hall S R. Biotemplated synthesis of an ordered macroporous superconductor with high critical current density using a cuttlebone template. *Chemical Communications*, 2008, 1055–1057.

[30] Lee S J, Lee Y C, Yoon Y S. Characteristics of calcium phosphate powders synthesized from cuttlefish bone and phosphoric acid. *Journal of Ceramic Processing Research*, 2007, **8,** 427–430.

[31] Lee S J, Yoon Y S, Lee M H, Oh N S. Highly sinterable beta-tricalcium phosphate synthesized from eggshells. *Materials Letters*, 2007, **61**, 1279–1282.

[32] Jia X, Ma X, Wei D, Dong J, Qian W. Direct formation of silver nanoparticles in cuttlebone-derived organic matrix for catalytic applications. *Colloids and Surfaces A*: *Physicochemical and Engineering Aspects*, 2008, **330**, 234–240.

[33] Xu G L, Li H, Ma X Y, Jia X P, Dong J, Qian W P. A cuttlebone-derived matrix substrate for hydrogen peroxide/glucose detection. *Biosensors and Bioelectronics*, 2009, **25**, 362–367.

[34] Jia X P, Qian W P, Wu D J, Wei D W, Xu G L, Liu X J. Cuttlebone-derived organic matrix as a scaffold for assembly of silver nanoparticles and application of the composite films in surface-enhanced raman scattering. *Colloid and Surfaces B*: *Biointerfaces*, 2009, **68,** 231–237.

[35] Ogasawara W, Shenton W, Davis S A, Mann S. Template mineralization of ordered macroporous chitin-silica composites using a cuttlebone-derived organic matrix. *Chemistry of Materials*, 2000, **12**, 2835–2837.

[36] Prasitsilp M, Jenwithisuk R, Kongsuwan K, Damrongchai N, Watts P. Cellular responses to chitosan in vitro: The importance of deacetylation. *Journal of Materials Science*: *Materials in Medicine*, 2000, **11**, 773–778.

[37] Cadman J, Zhou S, Chen Y, Li Q. Topology optimization of cellular structures, learnt from cuttlefish. in Rodrigues H, Guedes J M, Fernandes P, Folgado J, Neves M M (Eds.), *Eighth World Congress on Structural and Multidisciplinary Optimization*, ISSMO, Lisboa, Portugal, 2009.

[38] Cadman J, Zhou S, Chen Y, Li W, Appleyard R, Li Q. Characterization of cuttlebone for a biomimetic design of cellular structures. *Acta Mechanica Sinica*, 2010, **26**, 27–35.

[39] Bendsoe M P, Kikuchi N. Generating optimal topologies in structural design using a homogenization method. *Computer Methods in Applied Mechanics and Engineering*, 1988, **71**, 197–224.

[40] Song Y S, Youn J R. Evaluation of effective thermal conductivity for carbon nanotube/polymer composites using control volume finite element method. *Carbon*, 2006, **44**, 710–717.

[41] Cadman J, Chen Y, Zhou S, Li Q. Creating biomaterials inspired by the microstructure of cuttlebone. *Materials Science Forum*, 2010, **654-656**, 2229–2232.

[42] Cadman J, Chen Y, Zhou S, Li Q. Assessing the effects of natural variations in microstructure for the biomimetic modeling of cuttlebone. *Advanced Materials Research*, 2010, **123-125**, 295–298.

[43] Bensoussan A, Papanicolaou G, Lions J L. *Asymptotic Analysis for Periodic Structures*, North Holland Pub Co, Amsterdam, Holland, 1978.

[44] Torquato S, Hyun S, Donev A. Multifunctional composites: optimizing microstructures for simultaneous transport of

heat and electricity. *Physical Review Letters*, 2002, **89**, 266601.

[45] Gibiansky L V, Sigmund O. Multiphase composites with extremal bulk modulus. *Journal of the Mechanics and Physics of Solids*, 2000, **48**, 461–498.

[46] Zhou S, Li Q. Design of graded two-phase microstructures for tailored elasticity gradients. *Journal of Materials Science*, 2008d, **43**, 5157–5167.

[47] De Kruijf N, Zhou S W, Li Q, Mai Y W. Topological design of structures and composite materials with multiobjectives. *International Journal of Solids and Structures*, 2007, **44,** 7092–7109.

[48] Chen Y H, Zhou S W, Li Q. Computational design for multifunctional microstructural composites. *International Journal of Modern Physics B*, 2009, **23**, 1345–1351.

[49] Zhou S W, Li Q. A variational level set method for the topology optimization of steady-state Navier-Stokes flow. *Journal of Computational Physics*, 2008g, In Press.

[50] Jung Y, Torquato S. Fluid permeabilities of triply periodic minimal surfaces. *Physical Review E*, 2005, **72**, 056319.

[51] Zhou S W, Li Q. A microstructure diagram for known bounds in conductivity. *Journal of Materials Research*, 2008a, **23**, 798–811.

[52] Hashin Z, Shtrikman S. A variational appraoch to the theory of elastic behaviour of multiphase materials. *Journal of the Mechanics and Physics of Solids*, 1963a, **11**, 127–140.

[53] Milton G W, Kohn R V. Variational bounds on the effective moduli of anisotropic composites. *Journal of the Mechanics and Physics of Solids* 1988, **36,** 597–629.

[54] Hutmacher D W, Sittinger M, Risbud M V. Scaffold-based tissue engineering: rationale for computer-aided design and solid free-form fabrication systems. *Trends in Biotechnology*, 2004, **22**, 354–362.

[55] Liu C Z, Czernuszka J T. Development of biodegradable scaffolds for tissue engineering: a perspective on emerging technology. *Materials Science and Technology*, 2007, **23**, 379–391.